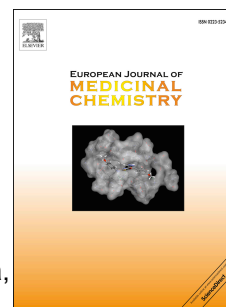# Accepted Manuscript

Design and synthesis of novel chalcones as potent selective monoamine oxidase-B inhibitors

Arwa Hammuda, Raed Shalaby, Stefano Rovida, Dale E. Edmondson, Claudia Binda, Dr. Ashraf Khalil

Please cite this article as: A. Hammuda, R. Shalaby, S. Rovida, D.E. Edmondson, C. Binda, A. Khalil, Design and synthesis of novel chalcones as potent selective monoamine oxidase-B inhibitors, *European Journal of Medicinal Chemistry* (2016), doi: 10.1016/j.ejmech.2016.02.038.

Design and synthesis of novel chalcones as potent selective monoamine oxidase-B inhibitors

Arwa Hammuda[a], Raed Shalaby[a], Stefano Rovida[b],

Dale E. Edmondson[c], Claudia Binda[b], and Ashraf Khalil[a,*]

[a]College of Pharmacy, Qatar University, Doha, Qatar

[b]Department of Biology and Biotechnology, University of Pavia, Via Ferrata 1, 27100 Pavia, Italy

[c]Department of Biochemistry, Emory University School of Medicine, Atlanta, Georgia 30322, USA

* Corresponding author: Dr. Ashraf Khalil

Qatar University, College of Pharmacy

P.O. Box 2713

Doha, Qatar

E-mail: akhalil@qu.edu.qa

Tel: +974-44035579

Abstract

A novel series of substituted chalcones were designed and synthesized to be evaluated as selective human MAO-B inhibitors. A combination of either methylsulfonyl or trifluoromethyl substituents on the aromatic ketone moiety with a benzodioxol ring on the other end of the chalcone scaffold was investigated. The compounds were tested for their inhibitory activities on both human MAO-A and B. All compounds appeared to be selective MAO-B inhibitors with K_i values in the micromolar to submicromolar range. Molecular modeling studies have been performed to get insight into the binding mode of the synthesized compounds to human MAO-B active site.

Keywords

Monoamine oxidase, neuroprotection, drug design, synthesis, enzyme, chalcones.
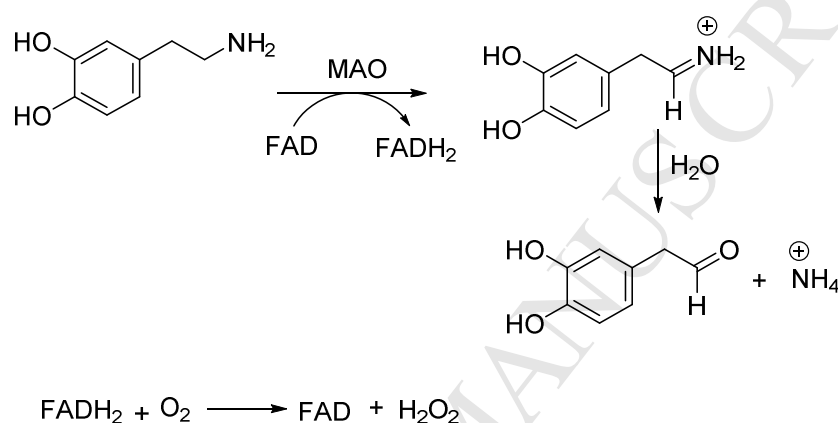
1. Introduction

Monoamine oxidases (MAO[1], EC 1.4.3.4) are mitochondrial membrane-bound, flavin-dependent enzymes responsible for the metabolism of arylalkylamine neurotransmitters (epinephrine, norepinephrine, β-phenylethylamine, serotonin and dopamine)[1] and a variety of xenobiotic amines[2] in the CNS and peripheral tissues by catalyzing their oxidative deamination to the corresponding aldehydes (Fig. 1). Two MAO isoforms (MAO-A and MAO-B) have been identified based on substrate specificity, inhibitor selectivity[3], amino acid sequence and tissue distribution.[4] MAO-A preferentially catalyzes the deamination of serotonin, epinephrine and norepinephrine and is specifically inhibited by clorgyline, while MAO-B preferentially oxidizes β-phenylethylamine and benzylamine and is inhibited by L-deprenyl. Both isoforms are active towards dopamine and tyramine.[5] The well-known role of MAOs in the metabolism of biogenic amines in neuronal tissues makes these enzymes important drug targets for diseases such as depression and Parkinson's disease.

Currently, the Protein Data Bank contains more than 40 crystal structures of MAO (most of them MAO-B) in complex with different reversible and irreversible inhibitors with resolutions ranging from 1.6 to 3 Å.[6] MAO-A and MAO-B share 70% sequence identity and a similar overall fold topology with the main differences consisting in details of the respective active sites, which accounts for their divergence in substrate and inhibitor specificity. The availability of such structural data paved the way for rationalized drug design of isoform-selective MAO inhibitors. Targeting MAO-A exerts an

---

[1] Abbreviations: MAO, monoamine oxidase; MMTP, 1-methyl-4-(1-methylpyrrol-2-yl)-1,2,3,6-tetrahydropyridine; MMDP$^+$, 1-methyl-4-(1-methylpyrrol-2-yl)-dihydropyridinium cation

antidepressant effect, while selective MAO-B inhibitors are being used to treat Parkinson's disease.[7] In addition, the MAO-catalyzed deamination reactions produce hydrogen peroxide as a byproduct (Fig. 1), which contributes to the oxidative stress condition typical of many pathologies. In this regard, MAO inhibitors are considered to act as neuroprotective agents in degenerative processes. [5, 8, 9]

Figure 1- MAO-catalyzed oxidative deamination of dopamine to 3,4-dihydroxyphenylacetaldehyde with the production of hydrogen peroxide as a byproduct

Based on the finding that MAO-B expression in neuronal tissue increases about 4-fold with age especially in glial cells[10], interest has increased in developing selective MAO-B inhibitors for neurodegenerative diseases. The majority of known MAO-B inhibitors act in an irreversible manner by forming a N(5)-flavocyanine adduct with the enzyme leading to potential immunogenicity effects in addition to long-lasting enzyme inhibition[11]. For this reason, over the last years, drug design studies have been focused on the development of reversible inhibitors that are devoid of these disadvantages, such as the recently approved new anti-Parkinson drug safinamide[12]. Along this line, new scaffolds have been explored including dihydropyrazoles[13],

4

chromones[14], coumarins[15], xanthines[16], thiazolidindiones[17] and chalcones[18]. The last ones, which chemically correspond to *trans*-1,3-diphenyl-2-propen-1-ones, represent an interesting group of natural compounds that are abundant in fruits and vegetables and possess a wide range of biological activities such as, anti-inflammatory[19], antimalarial[20], antifungal[21], anticancer[22] and antidepressant activities.[23]. They are open chain flavonoids and act as precursors in the biosynthetic pathways of this plant secondary metabolites[24]. With their structure consisting of two aromatic rings linked through a three-carbon α,β-unsaturated carbonyl system (C_6-C_3-C_6), they possess the required structural features for selective binding to human MAO-B[18, 25]. In this study, we report the synthesis of a series of novel chalcones that proved promising in terms of binding affinity and A/B isoform selectivity.

2. *Results and Discussion*

2.1. *Chemistry*

Ten novel chalcones were designed and prepared by Claisen-Schmidt condensation reaction of equimolar amounts of the appropriate substituted benzaldehydes and acetophenones in 1 mmol, 50% ethanolic NaOH solution as shown in Scheme-1.
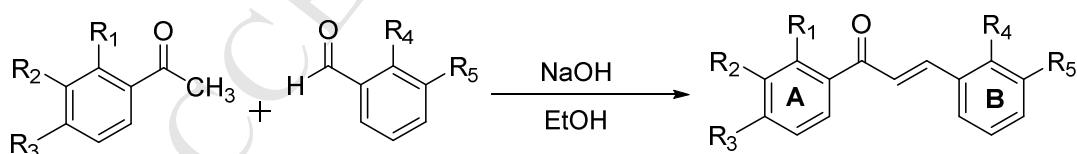
Scheme 1- Synthetic route to the selected chalcones

The filtered crude products were crystallized from ethanol to give crystalline compounds. The structures of the obtained compounds were confirmed by pertinent

spectroscopic techniques e.g. FT-IR, GC-MS and NMR. To assign the chemical shifts of all protons and carbons, compound-1 was subjected to 2D-NMR (HMQC and HMBC; Fig. 2). The olefinic protons appeared as doublet. The proton signal at δ 7.55 (J= 16 Hz) was assigned to the α-H and the carbon signal at δ 122.9 ppm to the α-C. While the proton signal at δ 8.12 (J= 16 Hz) and the carbon signal at δ 141 were assigned to the β-H and β-C respectively. The large coupling constant of the olefinic protons confirms the trans configuration.
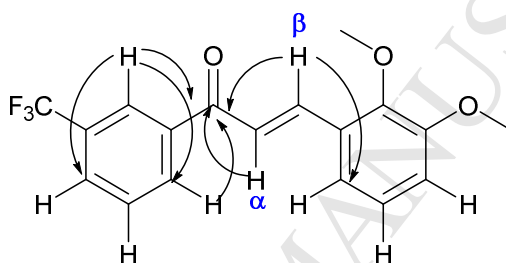
Figure 2 - Key HMBC correlations of compound 1

2.2. Biochemistry

The prepared compounds were screened for their inhibitory activities against human MAO-A and MAO-B at 10 μM final concentration by using an assay based on 1-methyl-4-(1-methylpyrrol-2-yl)-1,2,3,6-tetrahydropyridine (MMTP; Scheme 2) as substrate for both MAO isoforms (measured K_m values for human MAO-A and MAO-B are 88 μM and 101 μM, respectively, in agreement with previous reports [26-28]). The MAO-catalyzed oxidation of MMTP substrate is monitored at a wavelength (420 nm) that does not overlap with the inhibitor spectrum, therefore providing a direct and convenient assay for inhibition studies.

6
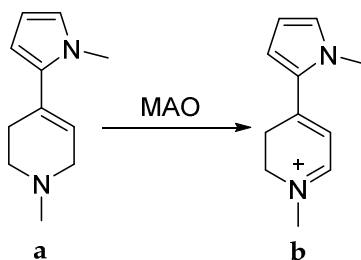
Scheme 2 - MAO-catalyzed oxidation of MMTP (**a**) to MMDP$^+$ (**b**)

Two series of chalcone derivatives were tested at a final concentration of 10 μM (Table 1). Derivatives **1-5**, which feature different substituents on the aromatic ketone moiety (A) and a dimethoxyphenyl ring (B) on the other end, showed poor MAO-B inhibition except for compound **3** and, in part, for **1**. Instead, the series **6-10** resulted to be more active, which suggests that the chalcone scaffold bearing a benzodioxol ring binds to human MAO-B with higher affinity than the dimethoxyphenyl moiety. In particular, the same substituent on ring A produces different inhibition effects when combined with either a methoxyphenyl or a benzodioxol units on ring B, as evinced by comparing **1** with **6**, **4** with **9** and **5** with **10**. The only exceptions are represented by a trifluoromethyl in *ortho* position that prevents binding in both cases (**2** and **7**) and a methylsulfonyl group in *para* that improves inhibition for either derivative (**3** and **8**). None of these molecules inhibits human MAO-A, except for a limited effect exerted by **6**.

Experiments to determine the IC$_{50}$ values were carried out on those compounds that showed a MAO-B inhibitory potency higher than 60% (**1**, **3**, **6**, **8**, **9**, **10**; Table 1). For all of them the IC$_{50}$ values are in the micromolar range with inhibitor **6** being the most active (IC$_{50}$ = 0.55 μM) and **1** the weakest (~ 8-fold less potent than **6**). A time-dependent analysis was performed by incubating MAO-B with compound **6** at a

7

concentration of 0.55 µM final concentration (IC$_{50}$) for varying periods of time (up to 1 hour) and measuring the residual enzymatic activity to investigate the binding mode of these class of molecules. The MAO-B residual enzymatic activity was unchanged at the various time points indicating that the inhibitory properties of **6** (and presumably those of the other compounds under investigation) are not time-dependent and do not involve any covalent adduct with either the flavin cofactor or protein residues (Fig. 3).
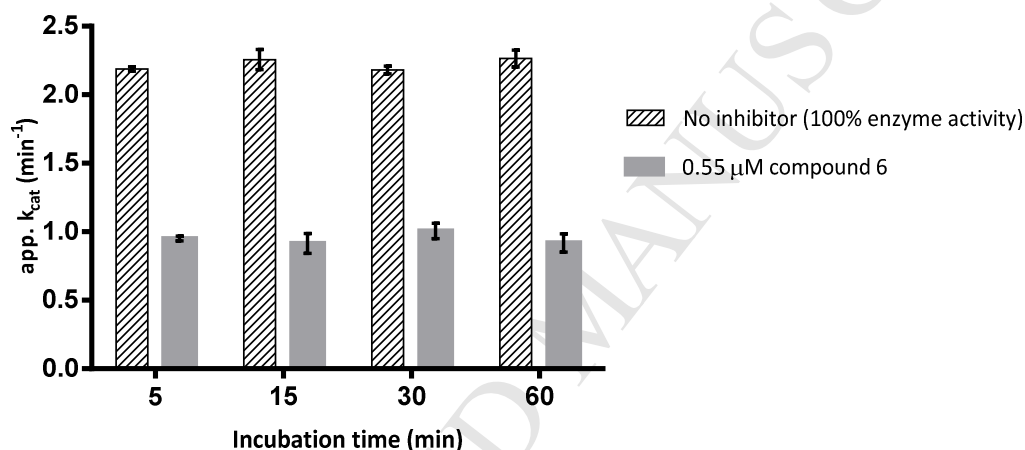
Figure 3 - Time-dependent inhibition of human MAO-B catalyzed oxidation of MMTP by compound **6**. The enzyme was preincubated for various periods of time (5 - 60 min) with **6** at 0.55 µM final concentration. The rates are expressed as apparent k$_{cat}$ values (min^{-1}). Error bars are shown and correspond to SEM from two replicates.

To investigate the inhibition of the most potent compounds in more detail and to provide a comparative analysis with other known MAO-B inhibitors, K$_i$ values were determined (Fig. 4) for compounds **3**, **6**, **8**, **9**, **10** (Table 1). The inhibition constants are approximately in line with the IC$_{50}$ values. Compound **9** represents the most potent inhibitor with a K$_i$ value of 0.55 µM, although **6** and **8** essentially inhibit MAO-B at a similar extent and even the inhibition constant for derivative 9 falls in the micromolar
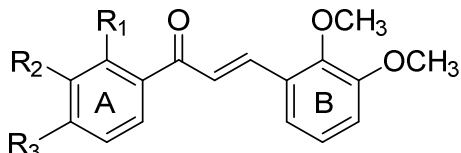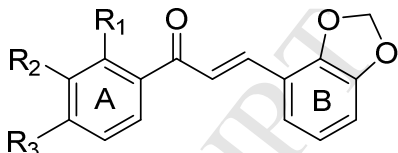
range. This suggests that any substituent on the ring A either at *meta-* or *para-* positions (but not in ortho- as in **7**) exerts a similar effect on the binding affinity to MAO-B. Instead, within series **1-5** a methylsulfonyl substituent (as in **3**) improves significantly the inhibitory potency with respect to the other substituents. Altogether, these observations suggest that a finely tuned combination of different chemical modifications on the ketone aromatic ring with a benzodioxol ring on the other end of the chalcone molecule leads to inhibitors with good human MAO-B binding affinity.
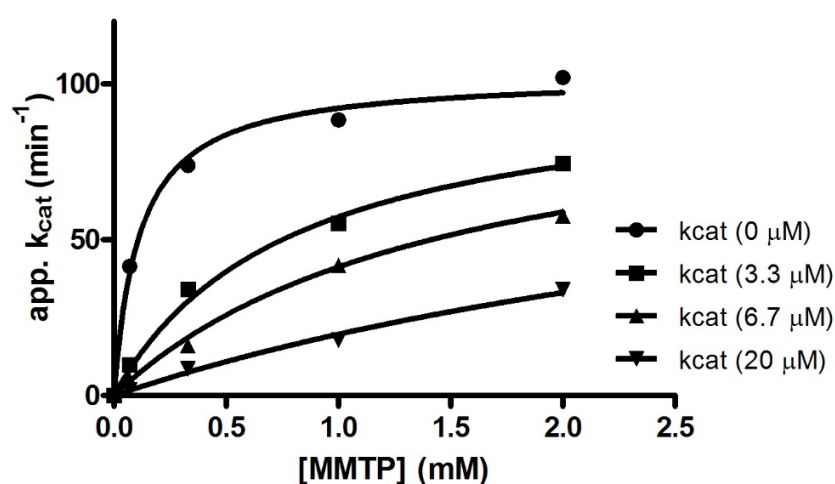
Figure 4 - Original curves for human MAO-B competitive inhibition by compound **9**. The inhibition constant (K_i) was determined by fitting the apparent k_{cat} values measured at varying MMTP substrate concentrations to the equation describing competitive inhibition: app. $k_{cat} = k_{cat} [S] / ([S] + K_m + K_m/K_i)$, where S is substrate concentration whereas k_{cat} and K_m are the steady-state parameters for each of the curves plotted at different inhibitor concentrations (inset in the plot) [29].

Table 1

Structures and human MAO inhibitory properties of the synthesized compounds.

1-5   6-10

| Compound | R_1 | R_2 | R_3 | MAO-B | | | MAO-A |
				Inhibition at 10 μM (%)	IC_{50} (μM)[a]	K_i (μM)	Inhibition at 10 μM (%)
1	H	CF_3	H	63	4.49 ± 0.03	n.d.[b]	0
2	CF_3	H	H	27	n.d.[b]	n.d.[b]	0
3	H	H	$CH_3\text{-}SO_2\text{-}$	90	1.97 ± 0.04	1.15 ± 0.12	0
4	H	H	$CH_3\text{-}S\text{-}$	36	n.d.[b]	n.d.[b]	0
5	H	$F_3C\text{-}O\text{-}$	H	41	n.d.[b]	n.d.[b]	0
6	H	CF_3	H	96	0.55 ± 0.07	0.78 ± 0.11	16
7	CF_3	H	H	7	n.d.[b]	n.d.[b]	n.d.[b]
8	H	H	$CH_3\text{-}SO_2\text{-}$	93	1.00 ± 0.07	0.72 ± 0.07	0
9	H	H	$CH_3\text{-}S\text{-}$	86	0.95 ± 0.07	0.55 ± 0.05	0
10	H	$F_3C\text{-}O\text{-}$	H	88	1.51 ± 0.05	2.36 ± 0.34	0

[a] All IC_{50} values shown in the table are the mean ± SEM from two experiments.

[b] n.d., not determined.

2.3. Molecular docking simulation

A docking simulation of the most active (**3**, **6**, **8**, **9**, **10**) among the synthesized compounds was performed to investigate their binding mode inside human MAO-B active site. In this enzyme either substrates or competitive inhibitors bind to a highly hydrophobic cavity that may exist as two entities: an "entrance cavity" separated from the outer surface by the cavity gating loop (residues 99–110), and a "substrate cavity"

10

that extends from FAD to the entrance cavity. Residues Tyr398 and Tyr435, together with FAD, form an "aromatic cage" where the catalyzed reaction occurs[30], while Ile199 plays an important role as a gating residue between the two cavities by adopting either a closed or an open conformation.[27] The docking simulation with compound **6** showed that the aromatic amino acids present in the binding site aid in the accommodation of the benzodioxol ring within the aromatic sandwich formed by Tyr398 and Tyr435, whereas ring A is directed towards the entrance cavity (Figs. 5 and 6). The same result was obtained with inhibitors **9** and **10** (Fig. 7), whereas compounds **3** and compound **8** are exceptions as they may adopt two major poses where the methylsulfonyl group is predicted to be either directed towards the substrate- or the entrance-cavity. This may be due to the ability of this group to form hydrogen bonds with Tyr398 and with the water molecules present in the aromatic cage (Fig. 8). This result predicts that the orientation of both rings mainly depends on the substituents and their ability to form binding contacts with the aromatic cage. In all poses the carbonyl oxygen anchors the inhibitors to the bottom of the binding site by forming hydrogen bond with Cys172. The position of the substituent on ring A was showed to be critical for inhibition, as it is favorable to be on *meta-* or *para-* position to be perfectly surrounded by the hydrophobic amino acids forming the entrance cavity (residues: Leu164, Leu167, Phe168 and Trp119). In contrast, substitution on *ortho-* position of ring A would cause a steric clash with carbonyl group that distorts the co-planar ring system and does not satisfy the appropriate distance between the carbonyl group as a hydrogen bond acceptor and the hydrophobic group. This may explain the lower activity of compound **2** and **7** compared to compound **1** and **6**.
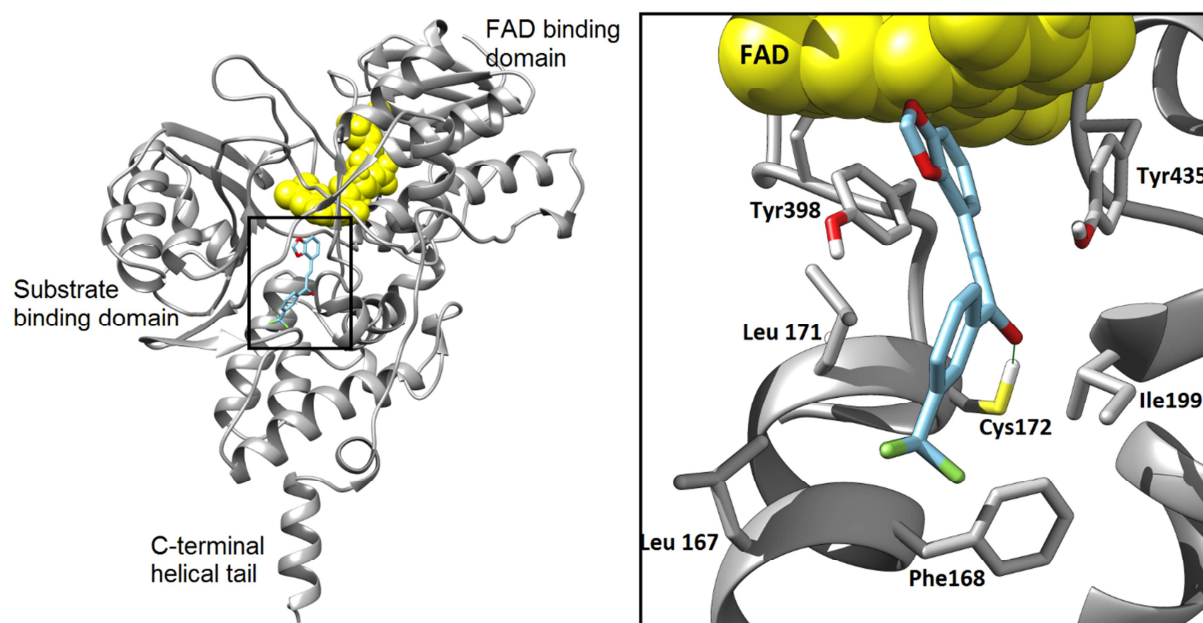
**Figure 5** - Ribbon stereoview of human MAO-B structure with the docked pose of compound **6** (stick representation), FAD is represented as yellow spheres. The inset shows a zoomed view of the active site highlighting the docked pose of compound **6** in MAO-B binding site with Ile199 adopting the open conformation. A hydrogen bond between Cys172 and carbonyl oxygen is shown as a green line.
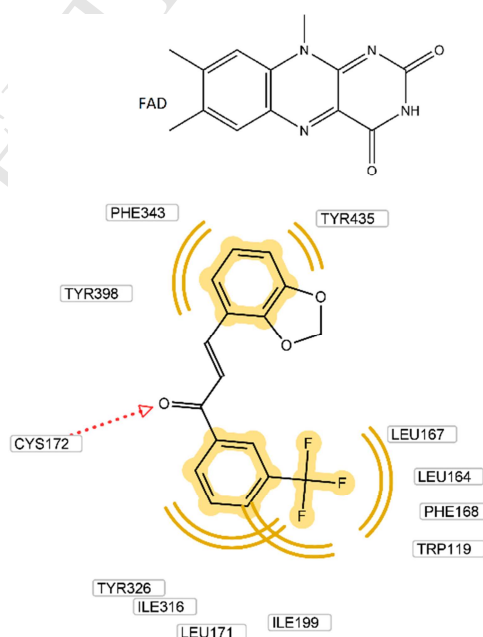
Figure 6 - 2D representation of the interactions of compound **6** with residues of human MAO-B binding site according to the docking results. The red arrow represents H-bond and yellow rings represent hydrophobic interactions. Key interacting amino acids are shown.
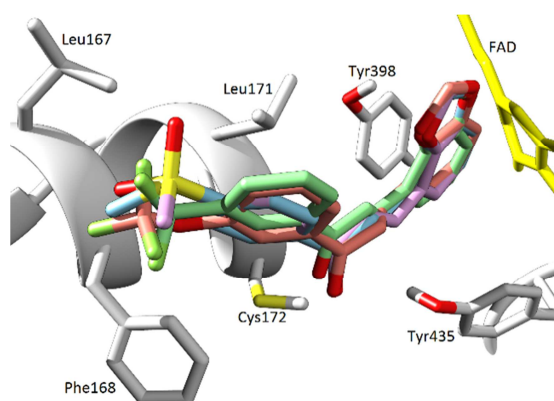
Figure 7 - Superimposition of docked poses of compounds 6 (green), 8 (purple), 9 (cyan) and 10 (pink) inside MAO-B binding site showing the same binding mode where ring A occupies the entrance cavity and ring B is directed towards FAD (yellow). Key interacting amino acids are shown in stick representation.
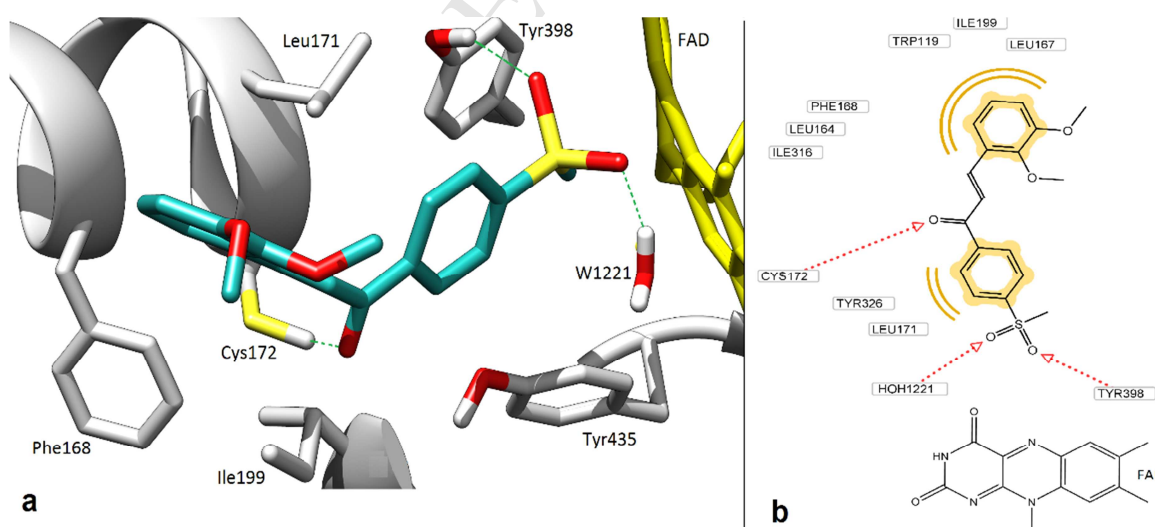
Figure 8 – a) The atypical binding mode of compound **3** inside MAO-B binding site as predicted by the docking calculations: ring A is directed towards FAD forming hydrogen bonds (green dashed lines) with Tyr398 and a water molecule. The methoxylated ring

occupies the entrance cavity. Key interacting amino acids are shown in stick representation. b) 2D representation of the atypical binding mode of compound 3 inside MAO-B binding site. The red arrows represent H-bonds and yellow rings represent hydrophobic interactions.

Conclusion

Chalcones are aromatic compounds which were shown to exert inhibitory properties on the MAO drug targets[18]. In this study, ten new chalcone analogs were evaluated for their activity on recombinant human MAO-A and B. The obtained data confirmed that all the prepared chalcone analogs are selective MAO-B inhibitors with negligible or no inhibitory activity on MAO-A, which is in agreement with previous studies[18, 25, 31]. In the present study a higher level of novelty was explored by introducing a benzodioxol ring in the molecule combined with different substituent on the other aromatic ring (Table 1). This is relevant considering that this chemical entity is present also in 3,4-methylenedioxymethamphetamine (the well-known illicit drug "ecstasy") which was showed to inhibit MAOs[32]. Our analysis revealed that the same substituent on the ketone aromatic ring exerts a different effect when combined with either a methoxyphenyl or a benzodioxol moiety, with the latter being more inhibitory.

The most active compounds were selected for further analyses, including both enzymatic assays to measure their inhibition potency and docking simulation to predict the binding mode. The inhibition of the chalcone derivatives is not time-dependent, indicating that their binding is reversible. The K_i values range from 0.55 to 2.36 μM with compound **9** being the most potent and having the same inhibition potency of the new anti-Parkinson drug safinamide[33]. These values are also comparable to those recently reported[34] for other chalcone derivatives, but a higher level of MAO-B/MAO-A selectivity was herewith achieved. In this regard, it is important to notice that the

14

hydrogen bond predicted to form between the inhibitor carbonyl oxygen and Cys172 is common to all the studied inhibitors. This protein residue is not conserved in human MAO A (corresponding to Asn181), which might represent an important element in determining isozyme selectivity[35]. The molecular docking simulation provided an explanation also for the crucial correlation between the inhibitory activity and the position of the substituent on the aromatic ketone ring, because it showed as either meta- or para- substitution would allow an inhibitor orientation perfectly surrounded by the hydrophobic active site residues. Moreover, an interesting result was obtained with compounds **3** and **8** that are predicted to bind in two opposite conformations including that with the methylsulphonyl-substituted ring within the MAO-B aromatic sandwich in front of the flavin ring. This observation will prompt further structural studies in order to investigate this aspect.

3. Experimental protocols

3.1. Materials and methods

All fine chemicals and solvents were obtained from Sigma–Aldrich (unless specified otherwise) and were used without further purification. For screening and IC_{50} determination, insect cell microsomes containing recombinant human MAO-A and MAO-B (5 mg/mL) from Sigma–Aldrich were used. For K_i measurements, recombinant human MAO-A and MAO-B were over-expressed in *Pichia pastoris* and purified as detergent-solubilized homogeneous samples by using published protocols .[27] Analytical thin layer chromatography was performed on precoated silica gel 60 F254 aluminum plates purchased from Fisher Scientific. Melting points were determined on a Stuart SMP40 automatic melting point apparatus and are uncorrected. All compounds

were analyzed for the presence of functional groups using Perkin Elmer Spotlight 400 Fourier transform infrared (FTIR) Imaging System. GC-MS analysis was performed on an Agilent 5973 GC/MS equipment. Proton (^{1}H) and carbon (^{13}C) NMR spectra were recorded on a Bruker Avance III spectrometer at 400 MHz using DMSO-d6 as a solvent or on a Jeol 500 in CDCl$_3$. Coupling constants are reported in hertz (Hz). The chemical shifts are reported as parts per million (δ) relative to the solvent peak. Purity of compounds were confirmed with C, H and S analysis performed on Thermo Scientific FLASH 2000 CHNS/O analyzer.

3.2. *Chemistry*

3.2.1. General Procedure for the synthesis of chalcones (1-10)

Chalcones were prepared utilizing Claisen-Schmidt condensation. To a stirred solution of the substituted acetophenone (1 mmol) and the substituted benzaldehyde (1 mmol) in ethanol at 0 ℃, sodium hydroxide solution (0.5 ml, 50%) was added dropwise. The solution was then stirred at room temperature overnight. The formed precipitate was filtered and washed with cold water and recrystallized from ethanol, to afford chalcones 1-10.

3.2.1.1. (*E*)-3-(2,3-dimethoxyphenyl)-1-(3-(trifluoromethyl)phenyl)prop-2-en-1-one (1)

Yellowish white solid, yield = 57%, m.p. = 84 – 88 ℃, ^{1}H NMR (400 MHz, CDCl$_3$) δ 8.42 (s, 1H, H$_2$), 8.18 (d, J = 7.8 Hz, 1H, H$_6$), 8.12 (d, J = 16 Hz, 1H, β-Olefinic), 7.83 (d, J = 7.8 Hz, 1H, H$_4$), 7.64 (dd, J = 8.2 Hz, 7.8 Hz, 1H, H$_5$), 7.55 (d, J = 16 Hz, 1H, α-Olefinic), 7.28 (dd, J= 7.1 Hz, 1.4 Hz, 1H, H$_{6'}$), 7.11 (dd, J= 7.8 Hz, 7.8 Hz, 1H, H$_{5'}$), 6.99 (dd, J= 7.6 Hz, 1.4 Hz, 1H, H$_{4'}$), 3.89 (s, 6H, -OCH$_3$). ^{13}C NMR (101 MHz, CDCl$_3$) δ 189.7, 152, 149, 141.1, 138, 131.8, 129.4, 129.2, 128, 125.5, 124, 123, 119.7, 114.6, 61.5, 56. Anal. calcd. for C$_{18}$H$_{15}$F$_3$O$_3$: C, 64.29; H, 4.50. Found: C, 64.79; H, 4.54. EI-MS (m/z): calculated 336.1, observed 336.1 (M).

3.2.1.2. (*E*)-3-(2,3-dimethoxyphenyl)-1-(2-(trifluoromethyl)phenyl)prop-2-en-1-one (2)

Buff solid, yield = 80%, m.p. = 63 - 66 ℃, ^{1}H NMR (400 MHz, DMSO-d$_6$) δ 7.91 (d, J = 7.7 Hz, 1H, H$_6$), [7.83 (dd, J = 7.3 Hz, 1H), 7.77 (dd, J = 7.6 Hz, 1H), H$_4$ and H$_5$], 7.68 (d, J = 7.4 Hz, 1H, H$_3$), 7.52 (d, J = 16.4 Hz, 1H, β-Olefinic), 7.45 (dd, J = 7.4, 1.6 Hz, 1H, H$_6$`), 7.24 (d, J = 16.4 Hz, 1H, α-Olefinic), 7.20 – 7.09 (m, 2H, H$_4$` and H$_5$`), 3.82 (s, 3H, -OCH$_3$), 3.65 (s, 3H, -OCH$_3$). ^{13}C NMR (101 MHz, DMSO-d$_6$) δ 188.23, 152.76, 148.44, 139.05, 138.29, 132.48, 130.14, 129.80, 129.48, 127.99, 125.27, 124.88, 124.29, 122.41, 119.30, 115.35, 61.06, 55.83. Anal. calcd. for $C_{18}H_{15}F_3O_3$: C, 64.29; H, 4.50. Found: C, 65.11; H, 4.46. EI-MS (m/z): calculated 336.1, observed 336.1 (M).

3.2.1.3. (*E*)-3-(2,3-dimethoxyphenyl)-1-(4-(methylsulfonyl)phenyl)prop-2-en-1-one (3)

Pale yellow solid, yield = 67%, m.p. = 171 - 175 ℃, ^{1}H NMR (400 MHz, DMSO-d$_6$) δ 8.35 (d, J = 8.3 Hz, 2H, H$_3$ and H$_5$), 8.11 (d, J = 8.3 Hz, 2H, H$_2$ and H$_6$), 8.04 (d, J = 15.8 Hz, 1H, β-Olefinic), 7.91 (d, J = 15.8 Hz, 1H, α-Olefinic), 7.64 (dd, J = 6.4, 2.8 Hz, 1H, H$_6$`), 7.25 – 7.10 (m, 2H, H$_4$` and H$_5$`), 3.85 (s, 3H, -OCH3), 3.81 (s, 3H, -OCH3), 3.31 (s, 3H, -SO$_2$CH$_3$). ^{13}C NMR (101 MHz, DMSO-d$_6$) δ 188.76, 152.78, 148.48, 144.19, 141.39, 139.25, 129.36, 127.92, 127.42, 124.36, 122.69, 119.30, 115.45, 61.07, 55.86, 43.21. Anal. calcd. for $C_{18}H_{18}O_5S$: C, 62.41; H, 5.24; S, 9.26. Found: C, 62.31; H, 5.27; S, 10.03. EI-MS (m/z): calculated 346.1, observed 346.1 (M).

3.2.1.4. (*E*)-3-(2,3-dimethoxyphenyl)-1-(4-(methylthio)phenyl)prop-2-en-1-one (4)

Pale yellow solid, yield = 83%, m.p. = 82 - 86 ℃, ^{1}H NMR (400 MHz, DMSO-d$_6$) δ 8.08 (d, J = 8.5 Hz, 2H, H$_2$ and H$_6$), 7.98 (d, J = 15.8 Hz, 1H, β-Olefinic), 7.88 (d, J = 15.8 Hz, 1H, α-Olefinic), 7.61 (dd, J = 9.0, 4.3 Hz, 1H, H$_5$`), 7.40 (d, J = 8.5 Hz, 2H, H$_3$ and H$_5$), 7.15 (d, J = 4.7 Hz, 2H, H$_4$` and H$_6$`), 3.84 (s, 3H, -OCH3), 3.79 (s, 3H, -OCH3), 2.55 (s, 3H, -S-CH3). ^{13}C NMR (101 MHz, DMSO-d$_6$) δ 188.01, 152.77, 148.25, 145.61, 137.65, 133.73, 129.03, 128.24, 124.96, 124.30, 122.73, 119.18, 114.96, 60.98, 55.81, 13.92. Anal. calcd. for $C_{18}H_{18}O_3S$: C, 68.77; H, 5.77; S, 10.20. Found: C, 68.97; H, 5.74; S, 11.25. EI-MS (m/z): calculated 314.1, observed 314.1 (M).

17

3.2.1.5. (*E*)-3-(2,3-dimethoxyphenyl)-1-(3-(trifluoromethoxy)phenyl)prop-2-en-1-one (5)

White solid, yield = 31%, m.p. = 81 - 84 ℃, ^{1}H NMR (400 MHz, DMSO-d$_6$) δ 8.19 (d, 1H), 8.09 – 7.99 (m, 2H), 7.9 (d, 1H), 7.77 – 7.60 (m, 3H), 7.21 – 7.10 (m, 2H), 3.83 (s, 3H, -OCH3), 3.79 (s, 3H, -OCH3). ^{13}C NMR (101 MHz, DMSO-d$_6$) δ 187.94, 152.76, 148.72, 148.43, 139.61, 138.95, 131.05, 127.99, 127.65, 125.55, 124.29, 122.39, 120.77, 119.28, 115.32, 61.03, 55.82. Anal. calcd. for $C_{18}H_{15}F_3O_4$: C, 61.39; H, 4.29. Found: C, 61.97; H, 4.32. EI-MS (m/z): calculated 352.1, observed 352.1 (M).

3.2.1.6. (*E*)-3-(benzo[d][1,3]dioxol-4-yl)-1-(3-(trifluoromethyl)phenyl)prop-2-en-1-one(6)

Deep yellow solid, yield = 45%, m.p. = 102 – 105 ℃ , 1H NMR (400 MHz, DMSO-d6) δ 8.36 (d, J = 7.8 Hz, 1H, H4), 8.31 (s, 1H, H2), 8.03 (d, J = 7.8 Hz, 1H, H6), 7.90 (d, J = 15.7 Hz, 1H, β-Olefinic), 7.82 (dd, J = 7.8 Hz, 1H, H$_5$), 7.74 (d, J = 15.7 Hz, 1H, α-Olefinic), 7.40 (d, J = 8.0 Hz, 1H, H$_6$`), 7.01 (d, J = 7.5 Hz, 1H, H4`), 6.92 (dd, J = 7.9 Hz, 1H, H5`), 6.18 (s, 2H, -O-CH2-O-). 13C NMR (101 MHz, DMSO-d6) δ 188.07, 147.69, 146.96, 138.46, 138.14, 132.34, 130.22, 129.52, 124.65, 122.93, 121.95, 121.86, 116.86, 110.39, 101.78. Anal. calcd. for $C_{17}H_{11}F_3O_3$: C, 63.76; H, 3.46. Found: C, 63.74; H, 3.41. EI-MS (m/z): calculated 320.1, observed 320.1 (M).

3.2.1.7. (*E*)-3-(benzo[d][1,3]dioxol-4-yl)-1-(2-(trifluoromethyl)phenyl)prop-2-en-1-one (7)

Yellow solid, yield = 62%, m.p. = 70 - 74 ℃, ^{1}H NMR (400 MHz, DMSO-d$_6$) δ 7.91 (d, J = 7.7 Hz, 1H, H$_6$), [7.84 (d, J = 7.5 Hz, 2H), 7.78 (d, J = 7.5 Hz, 2H), H$_4$ and H$_5$] 7.67 (d, J = 7.4 Hz, 1H, H$_3$), 7.26 (s, 2H, Olefinic), 7.20 (d, J = 7.8 Hz, 1H, H$_6$`), 7.03 (d, J = 7.6 Hz, 1H, H$_4$`), 6.90 (dd, J = 7.9 Hz, 1H, H$_5$`), 6.15 (s, 2H, -O-CH$_2$-O-). ^{13}C NMR (101 MHz, DMSO-d$_6$) δ 194.43, 147.74, 146.67, 141.33, 138.16, 132.60, 130.56, 128.30, 126.77, 122.35, 122.08, 116.30, 110.69, 101.84.Anal. calcd. for $C_{17}H_{11}F_3O_3$: C, 63.76; H, 3.46. Found: C, 64.39; H, 3.53. EI-MS (m/z): calculated 320.1, observed 320.1 (M).

3.2.1.8. (*E*)-3-(benzo[d][1,3]dioxol-4-yl)-1-(4-(methylsulfonyl)phenyl)prop-2-en-1-one (8)

Yellow solid, yield = 45%, m.p. = 126 - 130 ℃, ^{1}H NMR (400 MHz, DMSO-d$_6$) δ 8.27 (d, J = 7.4 Hz, 2H, H$_3$ and H$_5$), 8.13 (d, J = 7.3 Hz, 2H, H$_2$ and H$_6$), 7.85 (d, J = 15.6 Hz, 1H, β-Olefinic), 7.73 (d, J = 15.6 Hz, 1H, α-Olefinic), 7.37 (d, J = 7.4 Hz, 1H, H$_6$`), 7.03 (d, J = 7.0 Hz, 1H, H$_4$`), 6.94 (d, J = 7.4 Hz, 1H, H$_5$`), 6.20 (s, 2H, -O-CH$_2$-O-), 3.36 (s, 3H, -SO$_2$-CH3). ^{13}C NMR (101 MHz, DMSO-d$_6$) δ 188.85, 147.72, 146.93, 144.17, 141.32, 138.94, 129.22, 127.52, 123.49, 122.18, 122.03, 116.85, 110.50, 101.82, 59.76, 43.24, 20.75, 14.08.Anal. calcd. for

18

$C_{17}H_{14}O_5S$: C, 61.81; H, 4.27; S, 9.70. Found: C, 61.67; H, 4.25; S, 8.87. EI-MS (m/z): calculated 330.1, observed 330.1 (M).

3.2.1.9. (*E*)-3-(benzo[d][1,3]dioxol-4-yl)-1-(4-(methylthio)phenyl)prop-2-en-1-one (9)

Greenish yellow solid, yield = 23%, m.p. = 83 – 87 °C, ^{1}H NMR (400 MHz, DMSO-d$_6$) δ 7.99 (d, J = 8.3 Hz, 2H, H$_2$ and H$_6$), 7.85 (d, J = 15.7 Hz, 1H, β-Olefinic), 7.66 (d, J = 15.7 Hz,1H, α-Olefinic), 7.39 (d, J = 8.3 Hz, 2H, H$_3$ and H$_5$), 7.32 (d, J = 7.7 Hz, 1H, H$_6$·), 6.99 (d, J = 7.5 Hz, 1H, H$_4$·), 6.90 (dd, J = 7.8 Hz, 1H, H$_5$·), 6.17 (s, 2H, -O-CH$_2$-O-), 2.54 (s, 3H, -S-CH3). ^{13}C NMR (101 MHz, DMSO-d$_6$) δ 187.87, 147.67, 146.66, 145.73, 137.34, 133.57, 128.87, 125.04, 123.45, 122.11, 121.97, 117.17, 110.10, 101.71, 13.93. Anal. calcd. for $C_{17}H_{14}O_3S$: C, 68.44; H, 4.73; S, 10.75. Found: C, 69.05; H, 4.87; S, 11.01. EI-MS (m/z): calculated 298.1, observed 298.1 (M).

3.2.1.10. (*E*)-3-(benzo[d][1,3]dioxol-4-yl)-1-(3-(trifluoromethoxy)phenyl)prop-2-en-1-one

(10)

Deep yellow solid, yield = 30%, m.p. = 80 - 84 °C, ^{1}H NMR (400 MHz, DMSO-d$_6$) δ 8.10 (d, J = 7.4 Hz, 1H, H$_6$), 7.94 (s, 1H, H$_2$), 7.85 (d, J = 15.7 Hz, 1H, β-Olefinic), 7.71 (d, J = 15.7 Hz, 1H, α-Olefinic), 7.68 (m, 2H, H$_4$ and H$_5$), 7.37 (d, J = 8.0 Hz, 1H, H$_6$·), 7.00 (d, J = 7.6 Hz, 1H, H$_4$·), 6.90 (dd, J = 7.9 Hz, 1H, H$_5$·), 6.16 (s, 2H, -O-CH$_2$-O-). ^{13}C NMR (101 MHz, DMSO-d$_6$) δ 187.84, 148.74, 147.69, 146.94, 139.48, 138.41, 131.15, 127.49, 125.56, 122.98, 121.95, 121.88, 121.35, 120.46, 116.87, 110.37, 101.78. Anal. calcd. for $C_{17}H_{11}F_3O_4$: C, 60.72; H, 3.30. Found: C, 60.42; H, 3.18. EI-MS (m/z): calculated 336.1, observed 336.1 (M).

3.2.1.11.

3.3. Biochemistry

3.3.1. MAO inhibition screening

All synthesized compounds were evaluated for their ability to inhibit the A and B isoforms of human MAO by a spectrophotometric assay in which MMTP was used as a non-selective substrate (see text above in paragraph 2.2) and whose MAO-catalyzed oxidation product (dihydropyridinium species) was monitored by measuring absorbance

at 420 nm with a microplate and cuvette reader (SpectraMax M2, Molecular Devices). Due to their limited aqueous solubility, compounds 1-10 were dissolved in DMSO whose final concentration of 3.3% (v/v) which does not affect MAO activity. Control experiments were carried out in absence of the tested compound and adding an equal volume of DMSO to assure constant conditions in all measurements. Each assay was performed in a quartz cuvette containing 0.1 M potassium phosphate buffer (150 µL total volume) in which 25 µg of human MAO-A or MAO-B was incubated with 10 µM inhibitor at 37 °C for 5 minutes. The reaction was started by adding MMTP at a concentration of 0.15 mM. The increase in absorbance was recorded at 420 nm at 37 °C and the enzyme initial velocity (v_0) was calculated by using the extinction coefficient of 25000 M^{-1} cm^{-1}. The ratio between the v_0 value determined for each chalcone derivative and that in the control experiment (100% activity) was used to comparatively evaluate the inhibitory power of the tested compounds (Table 1). For those molecules that produced more than 60% of enzyme inhibition further experiments at different concentrations were carried out to determine IC_{50} by fitting the remaining activities (%) at different inhibitor concentrations [I] with respect to the reference assay (100%) as a function of log_{10}[I] in a dose-response curve with the Graphpad Prism 5.0 software.

3.3.2. Determination of the mode of inhibition of MAO-B

To investigate the mode of inhibition of the synthesized compounds, compound **6** (the most potent inhibitor in the presented study) was incubated with human MAO-B at a concentration of 0.55 µM (IC_{50}) for different times (5, 15, 30 and 60 minutes) and the enzymatic activity was measured as indicated above.

3.3.3 Determination of Ki for the most potent compounds

Further analysis to determine K_i was carried out by selecting the chalcone derivatives whose IC_{50} values were below 2 µM (Table 1). For these experiments purified samples of recombinant human MAO B were used with the reaction buffer containing also 0.25% v/v of reduced Triton X-100. The same MMTP assay as that described above was followed and the time-courses of the reaction were measured in quartz cuvettes under aerobic conditions by using a Cary 100 UV/Vis spectrophotometer (Agilent) equipped with thermostated cell holder (T=25 °C). Varied concentrations (0.07-2.00 mM) of MMTP and of the inhibitor under analysis (range 3-40 µM) were tested. Apparent k_{cat} values (calculated for each measurement as $v_0/[E]$, where v_0 is the initial velocity and [E] corresponds to enzyme concentration) were plotted as a function of substrate concentration and fit to equations describing competitive, uncompetitive, and noncompetitive inhibition patterns using Graphpad Prism 5.0 software. For all inhibitors the best fit was obtained with the equation of competitive inhibition and K_i values are reported in Table 1.

3.4. Molecular docking simulation

A molecular docking study was performed on the synthesized compounds to gain more insight of the binding mode with human MAO-B active site. The total procedure was conducted using Autodock 4.2 software[36]. The crystal structure of human MAO-B in complex with a coumarin analog was obtained from the PDB (2v61)[33] and was used throughout the molecular modeling study. Of the MAO-B dimeric structure chain A was selected for this study and prepared by adding hydrogen atoms and partial charges keeping FAD in an oxidized state. By investigation of various x-ray structures of MAO-B

21

co-crystalized with different inhibitors, it was observed that there are some conserved water molecules in proximity of the FAD, that appear to be important for mediating interactions with the inhibitors.[30] They are involved in a network of hydrogen bonds which stabilize the ligand into the binding site. Nine conserved water molecules were therefore included in the docking process.[37] 3D structures of the synthesized compounds were built using Openbabel[38] then imported into Autodock software. All compounds were prepared by adding hydrogen atoms and Gasteiger partial charges followed by merging non-polar hydrogens. All single bonds of the compounds were considered rotatable during the docking simulation where residues of the binding site were considered rigid. To define the binding site, a grid box of 60, 60, and 60 points in x, y, and z directions was centered on N5 atom of FAD with grid spacing of 0.375 Å. A total of hundred Lamarckian genetic algorithm runs were conducted for each compound with the following parameters: population size: 150, number of evaluations: 2,500,000 and number of generations: 27,000, returning the pose with the best binding energy in the largest cluster. Key interactions between docked poses and binding site residues were identified using UCSF Chimera.[39]

Acknowledgments

providing the MMTP substrate. The 2D-NMR spectra were recorded by Professor Khalid

Elsayed, University of Louisiana at Monroe, USA.

Supporting Information Available

Analytical and spectral data for the 10 compounds.

References

[1]   Tipton, K.F.; Boyce, S.; O'Sullivan, J.; Davey, G.P.; Healy, J., Monoamine oxidases: certainties and uncertainties. *Curr Med Chem,* **2004**, *11*, (15), 1965-1982.
[2]   Benedetti, M.S. In *Fundam Clin Pharmacol*: France, **2001**; Vol. *15*, pp 75-84.
[3]   Geha, R.M.; Rebrin, I.; Chen, K.; Shih, J.C., Substrate and Inhibitor Specificities for Human Monoamine Oxidase A and B Are Influenced by a Single Amino Acid. **2001**.
[4]   Rodriguez, M.J.; Saura, J.; Billett, E.E.; Finch, C.C.; Mahy, N., Cellular localization of monoamine oxidase A and B in human tissues outside of the central nervous system. *Cell Tissue Res,* **2001**, *304*, (2), 215-220.
[5]   Youdim, M.B.H.; Edmondson, D.; Tipton, K.F., The therapeutic potential of monoamine oxidase inhibitors. *Nature Reviews Neuroscience,* **2006**, *7*, (4), 295-309.
[6]   Binda, C.; Mattevi, A.; Edmondson, D.E. In *Int Rev Neurobiol*; 2011 Elsevier Inc: United States, **2011**; Vol. *100*, pp 1-11.
[7]   Riederer, P.; Lachenmayer, L.; Laux, G., Clinical applications of MAO-inhibitors. *Curr Med Chem,* **2004**, *11*, (15), 2033-2043.
[8]   Kaludercic, N.; Mialet-Perez, J.; Paolocci, N.; Parini, A.; Di Lisa, F., Monoamine oxidases as sources of oxidants in the heart. *J Mol Cell Cardiol,* **2014**, *73*, 34-42.
[9]   Kaludercic, N.; Carpi, A.; Menabo, R.; Di Lisa, F.; Paolocci, N. In *Biochim Biophys Acta*; 2010 Elsevier B.V: Netherlands, **2011**; Vol. *1813*, pp 1323-1332.
[10]   Barnham, K.J.; Masters, C.L.; Bush, A.I., Neurodegenerative diseases and oxidative stress. *Nat Rev Drug Discov,* **2004**, *3*, (3), 205-214.
[11]   Carradori, S.; Silvestri, R., New Frontiers in Selective Human MAO-B Inhibitors. *J Med Chem,* **2015**, *58*, (17), 6717-6732.
[12]   Fabbri, M.; Rosa, M.M.; Abreu, D.; Ferreira, J.J., Clinical pharmacology review of safinamide for the treatment of Parkinson's disease. *Neurodegener Dis Manag,* **2015**.
[13]   Fioravanti, R.; Desideri, N.; Biava, M.; Proietti Monaco, L.; Grammatica, L.; Yanez, M., Design, synthesis, and in vitro hMAO-B inhibitory evaluation of some 1-methyl-3,5-diphenyl-4,5-dihydro-1H-pyrazoles. *Bioorg Med Chem Lett,* **2013**, *23*, (18), 5128-5130.
[14]   Gaspar, A.; Teixeira, F.; Uriarte, E.; Milhazes, N.; Melo, A.; Cordeiro, M.N.; Ortuso, F.; Alcaro, S.; Borges, F., Towards the discovery of a novel class of monoamine oxidase inhibitors: structure-property-activity and docking studies on chromone amides. *ChemMedChem,* **2011**, *6*, (4), 628-632.
[15]   He, X.; Chen, Y.Y.; Shi, J.B.; Tang, W.J.; Pan, Z.X.; Dong, Z.Q.; Song, B.A.; Li, J.; Liu, X.H., New coumarin derivatives: design, synthesis and use as inhibitors of hMAO. *Bioorg Med Chem,* **2014**, *22*, (14), 3732-3738.

[16]	Okaecwe, T.; Swanepoel, A.J.; Petzer, A.; Bergh, J.J.; Petzer, J.P., Inhibition of monoamine oxidase by 8-phenoxymethylcaffeine derivatives. *Bioorg Med Chem,* **2012**, *20*, (14), 4336-4347.

[17]	Binda, C.; Aldeco, M.; Geldenhuys, W.J.; Tortorici, M.; Mattevi, A.; Edmondson, D.E., Molecular Insights into Human Monoamine Oxidase B Inhibition by the Glitazone Anti-Diabetes Drugs. *ACS Med Chem Lett,* **2011**, *3*, (1), 39-42.

[18]	Chimenti, F.; Fioravanti, R.; Bolasco, A.; Chimenti, P.; Secci, D.; Rossi, F.; Yanez, M.; Orallo, F.; Ortuso, F.; Alcaro, S., Chalcones: a valid scaffold for monoamine oxidases inhibitors. *J Med Chem,* **2009**, *52*, (9), 2818-2824.

[19]	Mateeva, N.; Gangapuram, M.; Mazzio, E.; Eyunni, S.; Soliman, K.F.; Redda, K.K., Biological evaluation of synthetic chalcone and flavone derivatives as anti-inflammatory agents. *Med Chem Res,* **2015**, *24*, (4), 1672-1680.

[20]	Tadigoppula, N.; Korthikunta, V.; Gupta, S.; Kancharla, P.; Khaliq, T.; Soni, A.; Srivastava, R.K.; Srivastava, K.; Puri, S.K.; Raju, K.S.; Wahajuddin; Sijwali, P.S.; Kumar, V.; Mohammad, I.S., Synthesis and insight into the structure-activity relationships of chalcones as antimalarial agents. *J Med Chem,* **2013**, *56*, (1), 31-45.

[21]	Lahtchev, K.L.; Batovska, D.I.; Parushev, S.P.; Ubiyvovk, V.M.; Sibirny, A.A., Antifungal activity of chalcones: a mechanistic study using various yeast strains. *Eur J Med Chem,* **2008**, *43*, (10), 2220-2228.

[22]	Sharma, R.; Kumar, R.; Kodwani, R.; Kapoor, S.; Khare, A.; Bansal, R.; Khurana, S.; Singh, S.; Thomas, J.; Roy, B.; Phartyal, R.; Saluja, S.; Kumar, S., A Review on Mechanisms of Anti Tumor Activity of Chalcones. *Anticancer Agents Med Chem,* **2015**, *16*, (2), 200-211.

[23]	Guan, L.P.; Tang, L.M.; Pan, C.Y.; Zhao, S.L.; Wang, S.H., Evaluation of potential antidepressant-like activity of chalcone-1203 in various murine experimental depressant models. *Neurochem Res,* **2014**, *39*, (2), 313-320.

[24]	Go, M.L.; Wu, X.; Liu, X.L., Chalcones: an update on cytotoxic and chemoprotective properties. *Curr Med Chem,* **2005**, *12*, (4), 481-499.

[25]	Morales-Camilo, N.; Salas, C.O.; Sanhueza, C.; Espinosa-Bustos, C.; Sepulveda-Boza, S.; Reyes-Parada, M.; Gonzalez-Nilo, F.; Caroli-Rezende, M.; Fierro, A., Synthesis, Biological Evaluation, and Molecular Simulation of Chalcones and Aurones as Selective MAO-B Inhibitors. *Chem Biol Drug Des,* **2015**, *85*, (6), 685-695.

[26]	Bissel, P.; Bigley, M.C.; Castagnoli, K.; Castagnoli, N., Jr., Synthesis and biological evaluation of MAO-A selective 1,4-disubstituted-1,2,3,6-tetrahydropyridinyl substrates. *Bioorg Med Chem,* **2002**, *10*, (9), 3031-3041.

[27]	Hubalek, F.; Binda, C.; Khalil, A.; Li, M.; Mattevi, A.; Castagnoli, N.; Edmondson, D.E., Demonstration of isoleucine 199 as a structural determinant for the selective inhibition of human monoamine oxidase B by specific reversible inhibitors. *J Biol Chem,* **2005**, *280*, (16), 15761-15766.

[28]	Yu, J.; Castagnoli, N., Jr., Synthesis and MAO-B substrate properties of 1-methyl-4-heteroaryl-1,2,3,6-tetrahydropyridines. *Bioorg Med Chem,* **1999**, *7*, (2), 231-239.

[29]	Copeland, R.A. *Enzymes: A Practical Introduction to Structure, Mechanism, and Data Analysis, 2nd Edition*, **2000**.

[30]	Ferino, G.; Vilar, S.; Matos, M.J.; Uriarte, E.; Cadoni, E., Monoamine oxidase inhibitors: ten years of docking studies. *Curr Top Med Chem,* **2012**, *12*, (20), 2145-2162.

[31]	Choi, J.W.; Jang, B.K.; Cho, N.C.; Park, J.H.; Yeon, S.K.; Ju, E.J.; Lee, Y.S.; Han, G.; Pae, A.N.; Kim, D.J.; Park, K.D., Synthesis of a series of unsaturated ketone derivatives as selective and reversible monoamine oxidase inhibitors. *Bioorg Med Chem,* **2015**, *23*, (19), 6486-6496.

[32]	Matsumoto, T.; Maeno, Y.; Kato, H.; Seko-Nakamura, Y.; Monma-Ohtaki, J.; Ishiba, A.; Nagao, M.; Aoki, Y., 5-hydroxytryptamine- and dopamine-releasing effects of ring-substituted amphetamines on rat brain: a comparative study using in vivo microdialysis. *Eur Neuropsychopharmacol,* **2014**, *24*, (8), 1362-1370.

[33]   Binda, C.; Wang, J.; Pisani, L.; Caccia, C.; Carotti, A.; Salvati, P.; Edmondson, D.E.; Mattevi, A., Structures of Human Monoamine Oxidase B Complexes with Selective Noncovalent Inhibitors: Safinamide and Coumarin Analogs. *Journal of Medicinal Chemistry,* **2007**, *50*, (23), 5848-5852.

[34]   Mathew, B.; Mathew, G.E.; Ucar, G.; Baysal, I.; Suresh, J.; Vilapurathu, J.K.; Prakasan, A.; Suresh, J.K.; Thomas, A., Development of fluorinated methoxylated chalcones as selective monoamine oxidase-B inhibitors: Synthesis, biochemistry and molecular docking studies. *Bioorg Chem,* **2015**, *62*, 22-29.

[35]   Heuson, E.; Storgaard, M.; Huynh, T.H.; Charmantray, F.; Gefflaut, T.; Bunch, L., Profiling substrate specificity of two series of phenethylamine analogs at monoamine oxidase A and B. *Org Biomol Chem,* **2014**, *12*, (43), 8689-8695.

[36]   Morris, G.M.; Huey, R.; Lindstrom, W.; Sanner, M.F.; Belew, R.K.; Goodsell, D.S.; Olson, A.J., AutoDock4 and AutoDockTools4: Automated Docking with Selective Receptor Flexibility. *Journal of computational chemistry,* **2009**, *30*, (16), 2785-2791.

[37]   Distinto, S.; Yáñez, M.; Alcaro, S.; Cardia, M.C.; Gaspari, M.; Sanna, M.L.; Meleddu, R.; Ortuso, F.; Kirchmair, J.; Markt, P.; Bolasco, A.; Wolber, G.; Secci, D.; Maccioni, E., Synthesis and biological assessment of novel 2-thiazolylhydrazones and computational analysis of their recognition by monoamine oxidase B. *European Journal of Medicinal Chemistry,* **2012**, *48*, (0), 284-295.

[38]   O'Boyle, N.M.; Banck, M.; James, C.A.; Morley, C.; Vandermeersch, T.; Hutchison, G.R., Open Babel: An open chemical toolbox. *Journal of cheminformatics,* **2011**, *3*, 33.

[39]   Pettersen, E.F.; Goddard, T.D.; Huang, C.C.; Couch, G.S.; Greenblatt, D.M.; Meng, E.C.; Ferrin, T.E., UCSF Chimera--a visualization system for exploratory research and analysis. *J Comput Chem,* **2004**, *25*, (13), 1605-1612.

Highlights:

- Novel chalcone analogs were designed and synthesized as human MAO-B reversible inhibitors.
- The inhibitors bind with micromolar to submicromolar potency.
- The molecular scaffold determines high MAO-A/MAO-B selectivity.
- A double conformation in MAO-B active site is predicted by molecular docking.